J. Fluid Mech. (1970), *vol.* 43, *part* 4, *pp.* 771–783
Printed in Great Britain

Measurements and computations of flow in pipe bends

By M. ROWE
Engineering Department, University of Cambridge

(Received 29 December 1969 and in revised form 9 April 1970)

Measurements are given of the total pressure and yaw relative to the pipe axis of flow in various pipe bends attached to the end of a long straight pipe, for a pipe Reynolds number of $2{\cdot}36 \times 10^5$. The behaviour of the induced secondary flows is presented in detail. In a 180° bend it is found that, from the start of the bend, the secondary flows increase to a maximum and then decrease to a steady value. This effect is explained by relating the local total pressure gradient to the production of streamwise vorticity. The same flow mechanism is used to predict qualitatively the flow pattern in an S-bend in which it is found that the secondary flows cause a complete interchange of the slow moving wall fluid and the faster central core. Results of a computer program for calculating the secondary flow from a knowledge of the upstream velocity profile are included. Although real fluid effects, other than those causing the upstream velocity profile, are omitted from the computations, the measured flow pattern is reasonably well predicted in a long bend up to a bend angle of about 75°.

Introduction

The general character of fluid motion in a bend is well known (Goldstein 1938; Schlichting 1955). When the fluid enters a bend, a pressure gradient is set up to provide the necessary inward acceleration. If the flow has a non-uniform velocity, the pressure gradient is insufficient for the faster moving particles and more than sufficient for the slower ones. A secondary flow is therefore formed with the faster fluid moving to the outside of the bend and the slower fluid to the inside. Thus, in a pipe bend in the horizontal plane with a velocity profile that is initially axisymmetric, the resultant flow is helical in the upper and lower halves of the pipe.

If the bend has a constant radius and the pipe a constant cross-section and is sufficiently long, the curved flow eventually becomes fully developed, i.e. the velocities do not vary with distance along the pipe axis. Considerable work by many authors has been done on fully developed curved flow (e.g. Adler (1934), for laminar flow, and Itō (1959), for turbulent flow). The main object has been to find the excess pressure loss in a curved pipe compared with that in the equivalent length of straight pipe. This additional loss is due to the secondary flow continuously sweeping the faster moving fluid into regions close to the pipe wall where it is retarded. Less attention has been paid to the transition region before the flow becomes fully developed. Transition curved flows are the concern of this paper.

Squire (1954) found that, for the turbulent flow of air in a gradual pipe bend (pipe diameter, $d = 3\frac{1}{2}$ in., bend radius $R = 42$ in.), the curved flow did not become fully developed for about 120°. The transition region is therefore relatively long, and the excess pressure loss coefficient derived for a fully developed curved flow pattern cannot be applied. Percival (1958) showed that, in the transition region in a straight section following a bend, the pressure loss is greatly affected by the presence of residual secondary flow at the bend exit.

The initial development of the secondary flow in the transition region can be explained by the growth of a streamwise component of vorticity ξ given by the simple equation, $\xi = -2\theta\Omega$, where θ is the angular distance from the start of the bend, and Ω is the upstream vorticity component in the plane of the bend and perpendicular to the main flow. This result was first proved by Squire & Winter (1951), assuming an inviscid, incompressible steady flow.

Detra (1953) showed that this concept of the secondary flow increasing linearly with bend angle agrees well with experiment up to a bend angle of about 40°.

Hawthorne (1951) postulated that the secondary flow may become oscillatory at large bend angles. He showed that in the simple case of a linear total pressure gradient across the flow at the entry to the bend, the surfaces of constant total pressure rotate through an angle α given by

$$\frac{d}{R}\frac{\partial^2\alpha}{\partial\theta^2} = \cos\alpha.$$

Thus, if $\alpha = 0$ when $\theta = 0$, α oscillates between 0 and π with a period or bend angle for a complete oscillation of $2{\cdot}36\pi(d/R)^{\frac{1}{2}}$. Experimental results given by Eichenberger (1951) show reasonable agreement. Hawthorne (1961) also inferred that some oscillatory movement of the secondary flow will be present when the total pressure profile at the bend entry is axisymmetric. In interpreting measurements of the total pressure at intervals round a pipe bend, Squire (1954) concluded from the relative shape of the contours that, providing the total pressure remains constant along a streamline (true for inviscid flow), the secondary flow in the transition region is oscillatory, with the oscillations being damped out as the curved flow becomes fully developed.

The experiments described in this paper examine transition flows like those measured by Squire in more detail with the angle of yaw relative to the pipe axis being measured as well as total pressure. Computations based on an inviscid theory are also made to determine the extent to which inviscid theory will predict the flow pattern in a pipe bend from a knowledge of the velocity distribution at the start of the bend.

Experimental details

A set of wooden circular pipe bend sections was constructed to allow pipe bends of various configurations in the horizontal plane to be formed on the building block principle. The sections were carefully machined and sealed with a plastic coating to avoid warping. The pipe diameter and bend radius were the same as in Squire's experiments ($3\frac{1}{2}$ in. and 42 in. respectively). The sections were guided

together by brass dowels, and held tight by case fasteners. Steps at the joins were virtually eliminated. Small leaks were plugged with plasticine. To allow oil flow patterns of the flow at the pipe wall to be inspected the pipes were split along the horizontal diameter. The inside wall of the pipe was smoothed and painted matt black. Straight pipe sections were of smooth bore mild steel tube.

The flow at the pipe inlet had a fully developed axisymmetric turbulent velocity profile. This was produced by a centrifugal blower exhausting into a large plenum and thence via a bell-mouth to a long (69 pipe diameters) straight pipe rough enough to produce the desired profile. For all the experiments, the velocity at the centre of the pipe was 158 ft./sec and the Reynolds number based on the mean velocity was $2{\cdot}36 \times 10^5$.

In order that the flow measurements could be made within the pipe bends (Squire made his measurements at the open end of the pipe, adding on sections to increase the bend angle), curved and straight test sections were made from perspex blocks. A probe could be inserted between two rings of foam rubber pressed together. A smear of lanoline allowed the probe to move freely in all directions and maintained an air-tight seal. Total pressure measurements were made with a Pitot tube. Yaw measurements in the horizontal plane were made partly with a claw-type yawmeter with claws inclined at 120° (see Schulze, Ashby & Erwin 1952), and partly with a 'Conrad' yawmeter consisting of two tubes soldered together with their ends chamfered at 45°. Stainless steel hypodermic tubing (0·042 in. O.D., 0·028 in. I.D.) was used throughout.

The probes were short coupled to a Statham PM 5 TC unbonded strain gauge differential pressure transducer with its output recorded by an N.E.P. 1050 UV Recorder. Mechanical coupling of the vertical probe movement to the paper movement converted the recorder to an $X-Y$ plotter. The probe traverse mechanism was electrically driven to reduce experimentation time.

Pressure calibration was effected by comparing the oscillograph trace position periodically with the reading on an inclined water tube manometer placed in parallel. Errors due to pressure gradients in the flow were found to be small. Trends in the variation of yaw were established by traversing the yaw probe vertically with its axis tangential to the pipe axis. More exact values of yaw were then obtained by the more laborious method of nulling the probe at certain points. Corrections were made at these points for the effect of the local total pressure gradient in the horizontal direction. This was done by first nulling the probe at intervals across the horizontal diameter at the open end of the long straight pipe upstream of the bend where the flow was assumed to be straight. A connexion was thus established between the resulting probe yaw error and the known total pressure gradient. The estimated accuracy of the yaw measurements is approximately $\pm 0{\cdot}5°$.

Flow measurements in a 180° bend

Figure 1 shows the total pressure contours measured at intervals in a 180° pipe bend and in a straight section downstream of the bend. The contours are of the difference between the measured total pressure (P) and the static pressure at the

start of the bend (p_0) divided by the maximum velocity head at the start of the bend ($\frac{1}{2}\rho U^2_{\max}$). Figure 2 shows contours of yaw in the horizontal direction relative to the pipe axis at similar points in the bend and straight section. Because of the

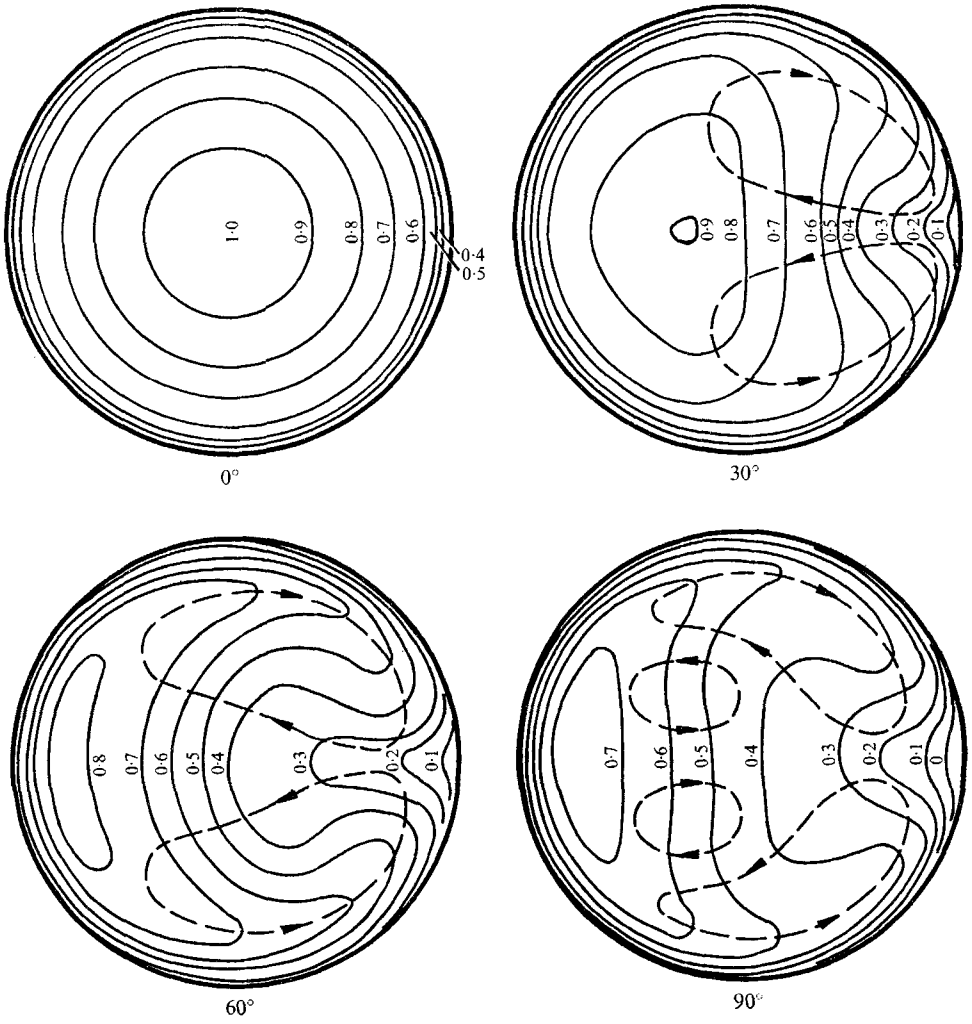

FIGURE 1. For legend see facing page.

symmetry noted by the pressure measurements, yaw measurements were made in the upper half of the pipe only and were assumed equal in the lower half. The yaw angles at the wall were taken from the direction of oil flow streak lines. The dashed yaw contours were estimated assuming secondary flow continuity over the pipe cross section.

The pressure contour plots are similar to those measured by Squire. The secondary flow displaces the position of the maximum total pressure towards the outside of the bend. At about 45° bend angle (this plot is given in figure 3), the contours appear most distorted when compared with their initial position. Measurements at 120°, 150° and 180° (not shown, but given by Rowe 1966)

indicate little change in contour shape after about 90°, i.e. the curved flow is by then fully developed. In the straight section, there is a gradual reversion to the profile for fully developed turbulent flow. The contours of yaw show that the

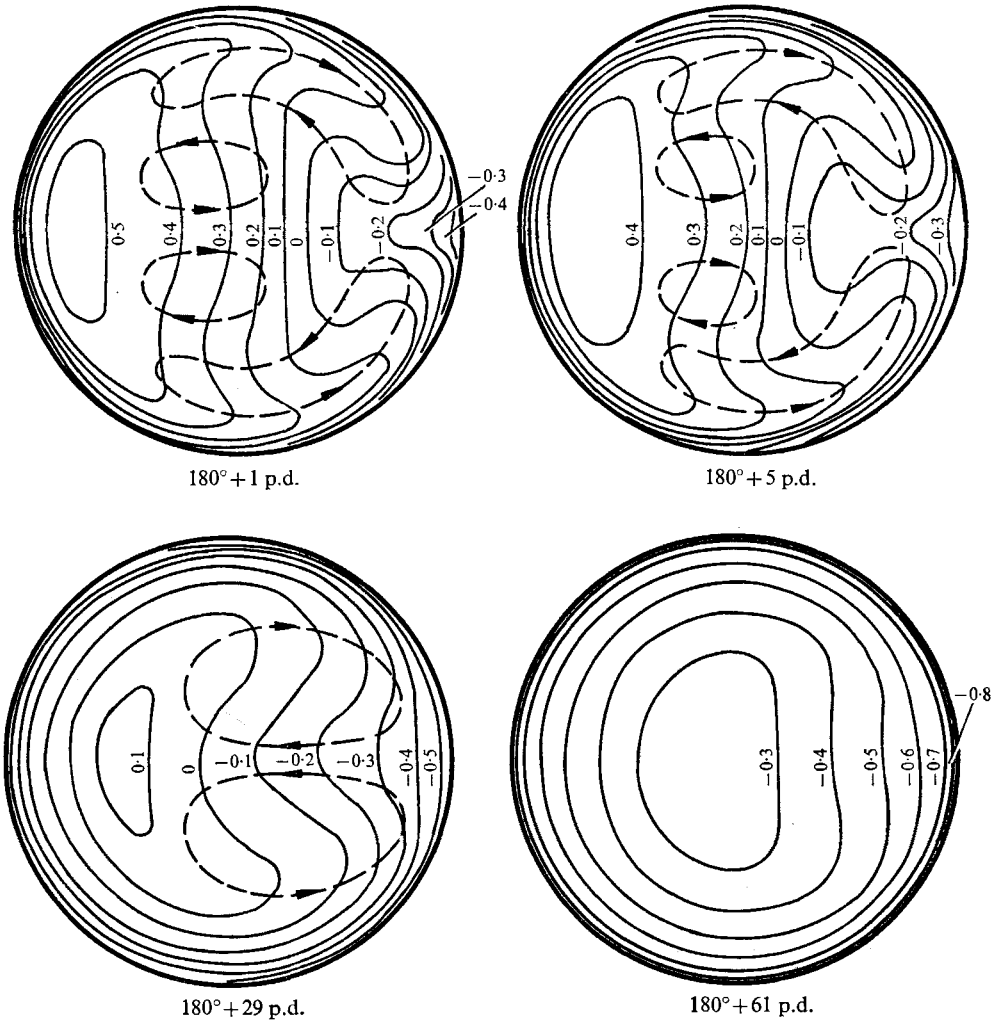

FIGURE 1. Contours of total pressure $(P-p_0)/\frac{1}{2}\rho U_{\max}^2$, in a 180° pipe bend and at various distances (pipe diameters) in a straight section downstream of the bend. The inside of the bend is to the right. Dashed lines show the estimated secondary flow pattern.

amount of secondary flow present is greatest at about 30° bend angle; after this the secondary flow is reduced. Downstream of the bend, the secondary flow persists for a considerable distance. Fluid yaw was measurable at the 29 pipe diameters station but could not be detected at 61 pipe diameters. The yaw measurements indicate some local reversal in secondary flow direction in the outer central region at about 90° (i.e. at point A, figure 2). The flow pattern in this region is difficult to define precisely as the flow angles are within the experimental accuracy. An estimate of the secondary flow pattern based on both the

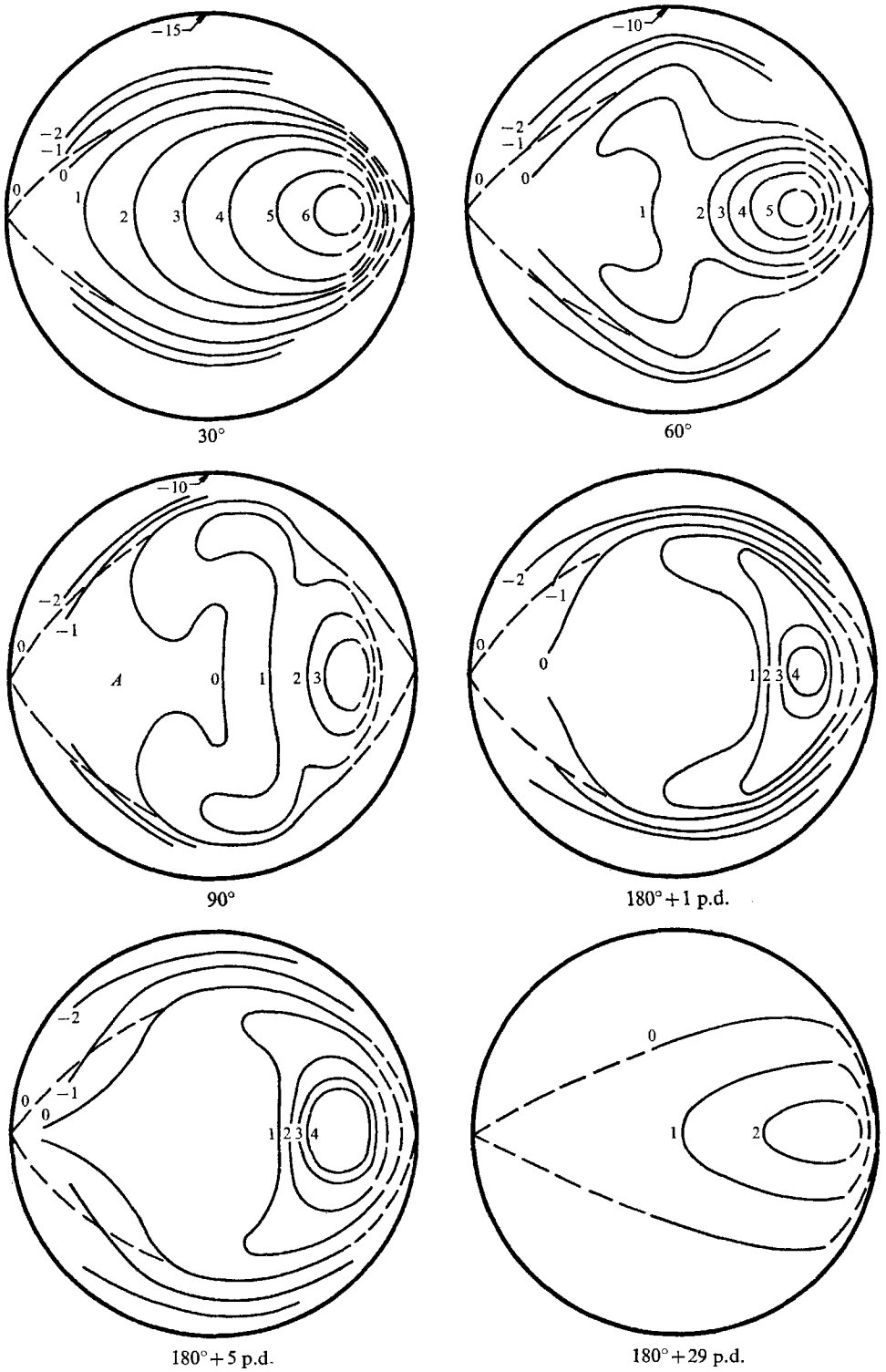

FIGURE 2. Contours of yaw (degrees from axis, positive outwards) in a 180° pipe bend and at various distances (pipe diameters) in a straight section downstream of the bend. Dashed lines are estimated assuming secondary flow continuity. The inside of the bend is to the right.

yaw measurements and the shape of the pressure contours is shown by the dashed lines in figure 1.

The reduction in flow after 30° can be explained by considering the shape of the total pressure contours at 45°. At position B in the first contour plot in

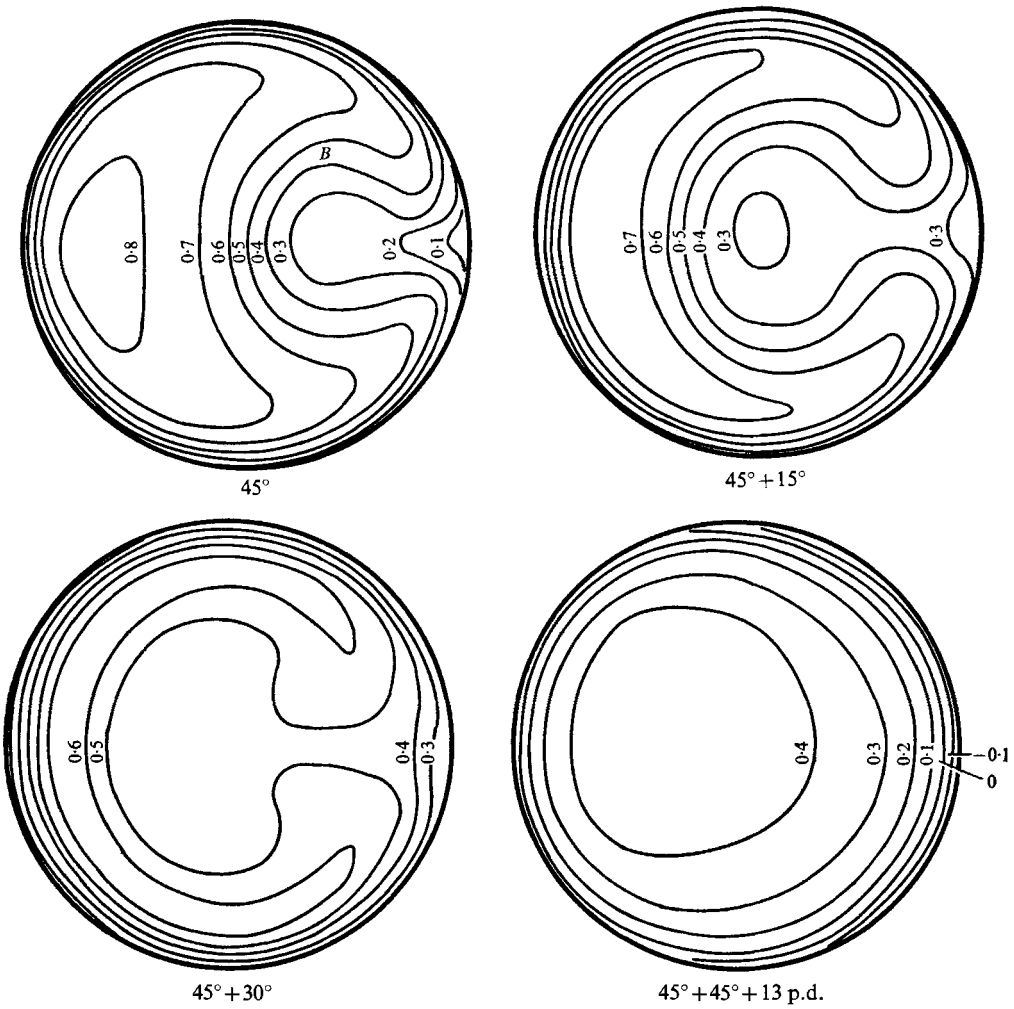

FIGURE 3. Contours of total pressure $(P-p_0)/\frac{1}{2}\rho U_{\max}^2$, in a 45°/45° S-bend and at 13 pipe diameters in a straight section downstream of the bend. The inside of the first 45° section is to the right.

figure 3, the total pressure gradient is such that, using the Squire & Winter result, a component of vorticity in the streamwise direction must be produced having the opposite sense of rotation to the streamwise vorticity produced at the start of the bend. The net result is a reduction in the total amount of secondary flow.

That the secondary flow appears to be concentrated largely at the inside of the bend may be explained in terms of the streamwise vorticity being generated continuously at the upper and lower wall and then being swept by the fluid

towards the inside of the bend. Here, the vorticity in the upper and lower halves of the pipe rolls up to form a vortex 'mangle', which shoots slow moving fluid at the inside wall into the centre of the pipe.

The fully developed curved flow pattern may be thought of as a balance between streamwise vorticity generated in both rotational senses in various parts of the flow field, streamwise vorticity which drifts with the flow and streamwise vorticity lost through viscous interaction and turbulent exchange.

Flow measurements in a 45°/45° S-bend

If the 180° bend is discontinued at the point in the bend where the shape of the pressure contours is starting to reduce the secondary flow (i.e. at about the 45° point), and a reverse bend is added, an initial increase in secondary flow is to be expected. This is because streamwise vorticity, will then be generated, according to the Squire & Winter result, in the *same* rotational sense as the secondary flow. That this supposition appears to be true can be seen from figure 3, which shows pressure contours in and downstream of a 45°/45° S-bend. The contour plot at 45° is taken from the measurements made in the 180° bend. If the contours at 45° + 15° in figure 3 are compared with those at 60° in figure 1, it can be seen that in the S-bend the zone of low-pressure fluid has now drifted to the centre of the pipe and is almost completely surrounded by higher pressure fluid. Downstream of the S-bend, this low-pressure 'bubble' is quickly filled and fully developed pipe flow is restored much sooner than after the 180° bend. (The contours 13 pipe diameters downstream of the S-bend in figure 3 are comparable in shape with those at 61 pipe diameters downstream of the 180° bend in figure 1.)

The complete interchange of slow moving wall fluid with the faster fluid in the central core that occurs in S-bends may well explain the substantial increase in the heat transfer rate between the walls and the fluid that is found in such cases. For instance, Remfry found an increase in heat transfer of 38 % in wavy pipes composed of 33° circular arcs compared with that in similar straight pipes.

Comparison with inviscid theory

In order to provide numerical prediction of the flow pattern in a pipe bend, a computer program was written which accepted a given velocity distribution at the start of the bend, then utilized the Squire & Winter result to calculate the secondary flow and the induced displacement of the total pressure contours in a step-by-step manner around the bend. The basic theory is as follows.

Consider secondary velocity components v and w in the plane of the bend and perpendicular to it, respectively (figure 4). Assuming that the secondary flow only causes a small displacement of the total pressure contours, one may write a continuity equation

$$\frac{\partial v}{\partial y} + \frac{\partial w}{\partial z} = 0$$

for the secondary flow. A secondary flow stream function ψ may be defined such

that $v = -\partial\psi/\partial z$ and $w = \partial\psi/\partial y$. Since ξ, the vorticity in the streamwise direction is given by

$$\xi = \frac{\partial w}{\partial y} - \frac{\partial v}{\partial z};$$

it follows from the Squire & Winter result, assuming $\Omega = \partial U/\partial z$, that

$$\frac{\partial^2\psi}{\partial y^2} + \frac{\partial^2\psi}{\partial z^2} = -2\theta\frac{\partial U}{\partial z}.$$

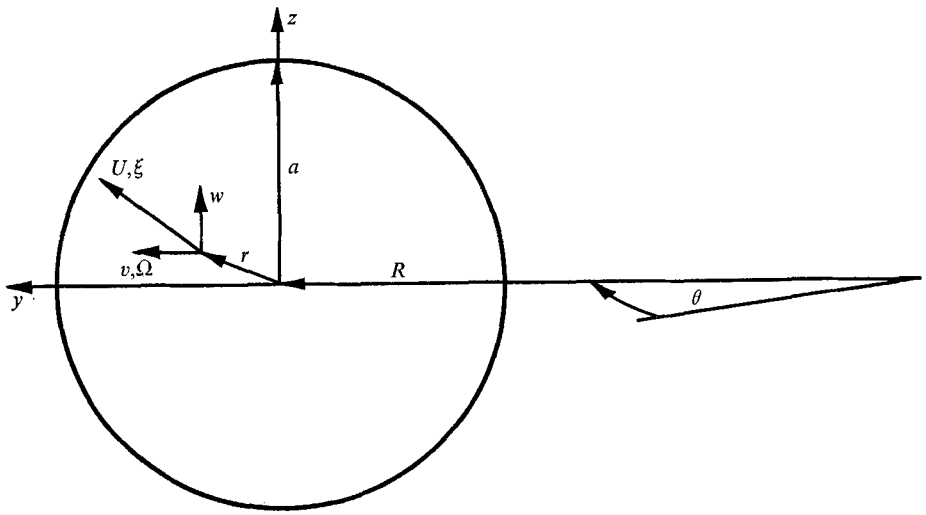

FIGURE 4. Bend co-ordinate system.

The computer program was built up as follows:

(i) A velocity profile $U = U_{\max}(1-r/a)^{\frac{1}{8}}$ was assumed at the start of the bend (this fitted the measured profile).

(ii) The Poisson equation for ψ was solved, numerically, at a number of points forming a grid placed across the upper half of the pipe at bend angle θ. A Gauss–Seidel method of relaxation was employed. ψ was assumed zero at the wall and along the horizontal diameter. Symmetry was assumed between the upper and lower halves of the pipe.

(iii) Secondary flow velocities were calculated at the grid points, and hence the streamline and total pressure contour shift, assuming secondary flow velocities which were the arithmetic mean of the initial and final values in the step.

(iv) The process was then repeated successively round the bend starting each step with the new computed axial velocity distribution (since only the gradient normal to the plane of the bend is required, in which direction there is no static pressure variation, this distribution can be found from the total pressure contours). The distribution of ξ at the end of a step was made to include that vorticity generated in the step according to the Squire & Winter result plus that vorticity which had been generated in all previous steps and had then drifted with the streamlines. The step length in the computations was 5°.

Complete details are given by Rowe (1966).

Figure 5 shows a comparison of the computed total pressure contours with experiment for a 90° bend. To make some allowance for real flow effects, the mean measured pressure loss at each station has been subtracted from the computed values. The last two plots in figure 5 show computed and measured yaw values.

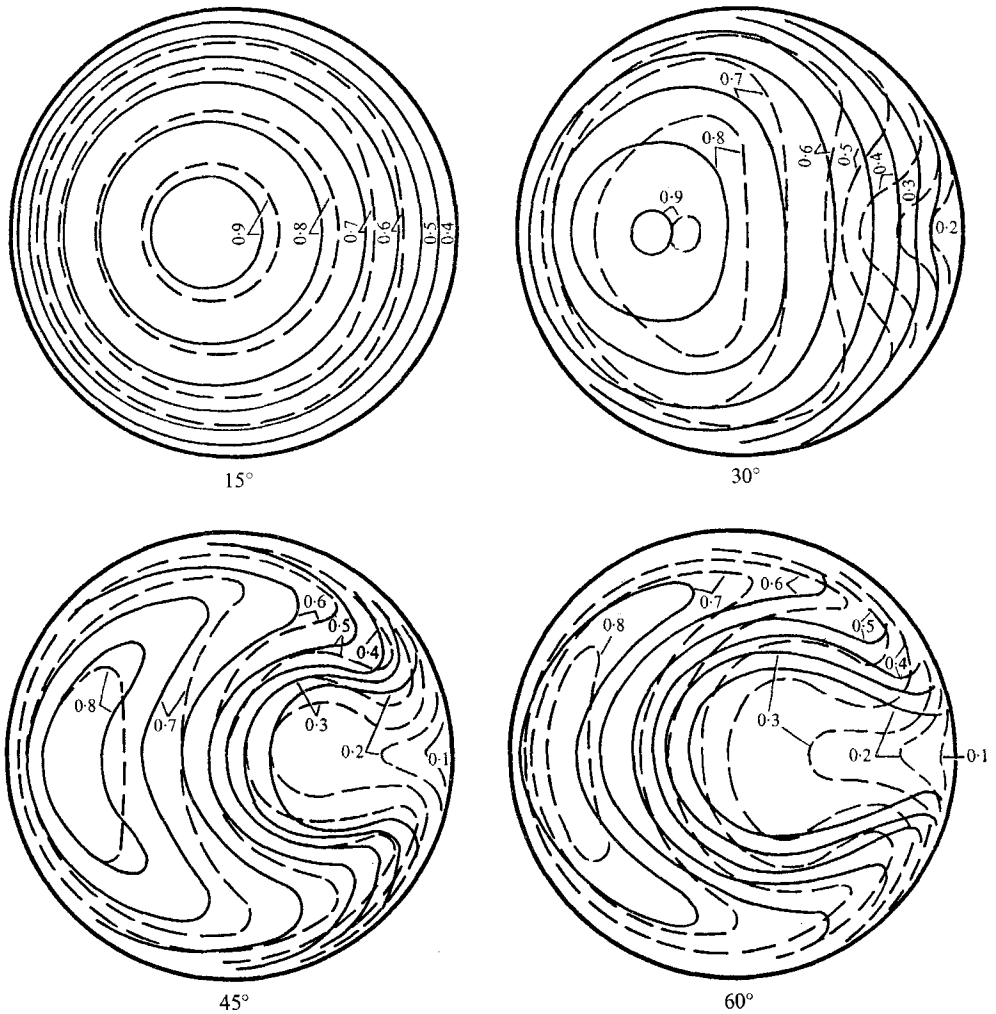

FIGURE 5. For legend see facing page.

The numerical computation procedure tended to break down at the region near the inside of the bend, mainly because of the difficulty of refining the grid pattern to cope with the large local variations in secondary flow in this region. Although limits were set to the calculated values, so that unrealistic values would not dominate the results in other regions, the region of uncertainty expanded until at 90°, the computed values were clearly incorrect over much of the cross section of the pipe. The computed contours agree in general shape with the measured values, although the computed inward movement of the low-pressure bubble tends to overshoot from 45° onwards (compare the measured and computed 0·3

pressure contours at 60° in figure 5), probably because the mathematical model contains no mechanism for vortex dissipation. Figure 6 shows computed and measured pressure contours in a 30°/30° S-bend. The tendency for the low-pressure bubble to spread over the centre of the pipe in an S-bend, and be

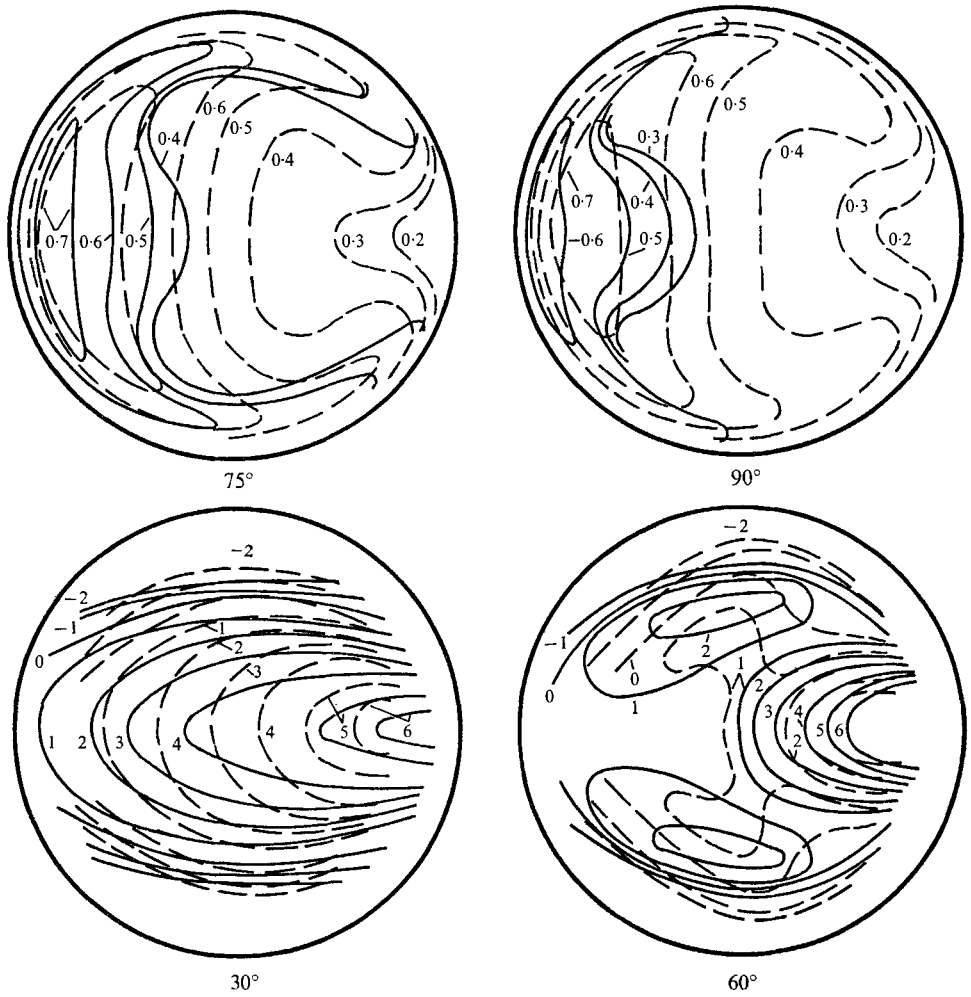

FIGURE 5. Computed (solid lines) and measured (dashed lines) total pressure and yaw (last two plots) in a 90° pipe bend. The inside of the bend is to the right.

surrounded by faster fluid is also reasonably well reproduced by the computations. (Compare the pressure contours at 60°, figure 5 with those at 30° + 30°, figure 6.)

Conclusion

Detailed measurements have been made of the flow pattern in transition regions in pipe bends before the curved flow pattern has become fully developed. In a long bend, the secondary flow caused by a fully developed straight pipe

profile at the start of the bend increases to a maximum at a bend angle of about 30°. From this point onwards, the total secondary flow is reduced until by about 90° it reaches a steady value. After this, the curved flow can be considered to be fully developed with no further change in the flow pattern.

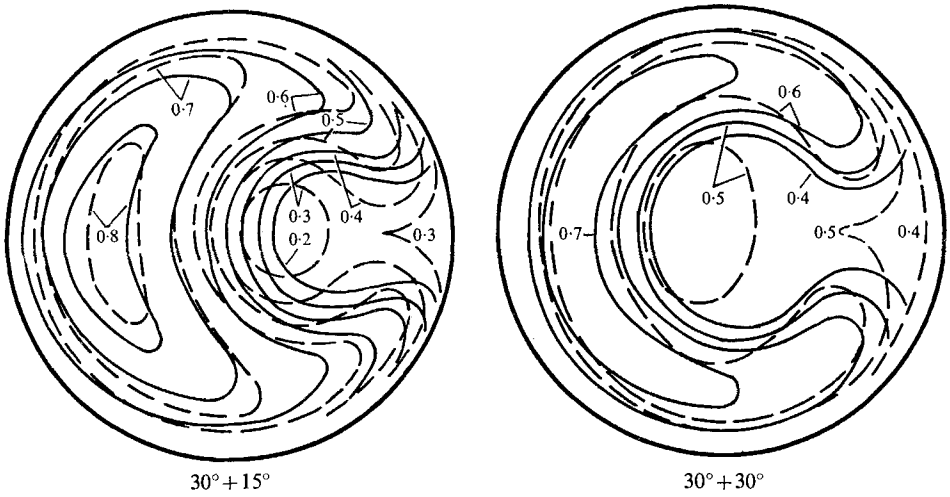

FIGURE 6. Computed (solid lines) and measured (dashed lines) total pressure in a 30°/30° S-bend. The inside of the first 30° bend is to the right.

It is shown that the Squire & Winter result of streamwise vorticity being produced whenever there is a total pressure gradient perpendicular to the plane of the bend is useful in predicting the secondary flow pattern further downstream. Thus, in the long bend, a mechanism for preventing the secondary flow increasing indefinitely, and for allowing the flow to become fully developed, is provided by the formation of total pressure gradients, opposite in sign to those at the start of the bend, and the consequent production of vorticity of opposite rotational sense. When the bend is reversed so that this negative vorticity becomes positive, the secondary flow tends to increase. This is evident in a 45°/45° S-bend in which the secondary flow causes a complete interchange of wall fluid and fluid in the central core, possibly indicating the reason why heat transfer effects are large in wavy pipes.

Reasonable agreement between numerical computations using the Squire & Winter result and the measured flow pattern has been shown up to a bend angle of about 75° and for a 30°/30° S-bend. The computations eventually break down because of the absence of any mechanism for vortex dissipation, and because of the practical difficulty of refining the numerical calculations to cope with regions having large local variations in secondary flow.

The author thanks Professor W. R. Hawthorne for his guidance in this study, and the Science Research Council for financial aid.

REFERENCES

ADLER, M. 1934 Strömung in gekrümmten Rohren. *Z. angew. Math. Mech.* **14**, 257–275.

DETRA, R. W. 1953 The secondary flow in curved pipes. E.T.H., Zurich, *Mitt. a. d. Inst. f. Aerodynamik*, no. 20.

EICHENBERGER, H. P. 1951 Shear flow in bends. M.Sc. Thesis, MIT.

GOLDSTEIN, S. 1938 *Modern Developments in Fluid Mechanics* (vols. 1, 2). Oxford University Press.

HAWTHORNE, W. R. 1951 Secondary circulation in fluid flow. *Proc. Roy. Soc.* A **206**, 374–387.

HAWTHORNE, W. R. 1961 Flow in bent pipes. *Proc. of Seminar in Aero. Sciences, Nat. Aero. Lab. Bangalore*, (pp. 305–333).

ITŌ, H. 1959 Friction factors for turbulent flow in curved pipes. *Trans. ASME*, D, **81**, 123–134.

PERCIVAL, P. M. E. 1958 Some problems in the rotational flow of fluids. Ph.D. Thesis, Cambridge University.

REMFRY, J. 1954 Heat transference and pressure loss for air flowing in passages of small dimensions. *Aero. Res. Counc., R. & M.* no. 2638.

ROWE, M. 1966 Some secondary flow problems in fluid dynamics. Ph.D. Thesis, Cambridge University.

SCHLICHTING, H. 1955 *Boundary Layer Theory*. New York: McGraw-Hill.

SCHULZE, W. M., ASHBY, G. C. & ERWIN, J. R. 1952 Several combination probes for surveying static and total pressure and flow distribution. *NACA TN* 2930.

SQUIRE, H. B. & WINTER, K. G. 1951 The secondary flow in a cascade of airfoils in a non-uniform stream. *J. Aero. Sci.* **18**, 271–277.

SQUIRE, H. B. 1954 Note on secondary flow in a curved circular pipe. *Aero. Res. Counc., Rep.* no. 16601.